# Regulatory and Essential Light Chains of Myosin Rotate Equally during Contraction of Skeletal Muscle

Julian Borejdo, Dmitry S. Ushakov, and Irina Akopova
Department of Molecular Biology and Immunology, University of North Texas, Fort Worth, Texas 76107-2699 USA

ABSTRACT Myosin head consists of a globular catalytic domain and a long $\alpha$-helical regulatory domain. The catalytic domain is responsible for binding to actin and for setting the stage for the main force-generating event, which is a "swing" of the regulatory domain. The proximal end of the regulatory domain contains the essential light chain 1 (LC1). This light chain can interact through the N and C termini with actin and myosin heavy chain. The interactions may inhibit the motion of the proximal end. In consequence the motion of the distal end (containing regulatory light chain, RLC) may be different from the motion of the proximal end. To test this possibility, the angular motion of LC1 and RLC was measured simultaneously during muscle contraction. Engineered LC1 and RLC were labeled with red and green fluorescent probes, respectively, and exchanged with native light chains of striated muscle. The confocal microscope was modified to measure the anisotropy from 0.3 $\mu m^3$ volume containing ~600 fluorescent cross-bridges. Static measurements revealed that the magnitude of the angular change associated with transition from rigor to relaxation was less than 5° for both light chains. Cross-bridges were activated by a precise delivery of ATP from a caged precursor. The time course of the angular change consisted of a fast phase followed by a slow phase and was the same for both light chains. These results suggest that the interactions of LC1 do not inhibit the angular motion of the proximal end of the regulatory domain and that the whole domain rotates as a rigid body.

## INTRODUCTION

Myosin subfragment-1 (S1) consists of the N-terminal, globular catalytic domain and the C-terminal, $\alpha$-helical regulatory domain. The catalytic domain is responsible for binding to actin and hydrolysis of ATP. The regulatory domain, which is stabilized by the essential and the regulatory light chains, is a long $\alpha$-helix extending toward the thick filaments. Atomic structure of S1 suggested that the regulatory domain may act as a "lever arm," translating small conformational changes occurring in the catalytic domain due to ATP hydrolysis, to a large linear motion of the thick filaments (Rayment et al., 1993). Consistent with this view, the regulatory domain rotated in response to rapid photogeneration of ATP (Allen et al., 1996; Ling et al., 1996). After rapid tension release it rotated in synchrony with the power stroke (Sabido-David et al., 1998a,b; Hopkins et al., 1998; Corrie et al., 1999). Subsequent work suggested that the regulatory domain rotated around a pivot located in the catalytic domain (Burghardt et al., 1998; Dominguez et al., 1998). Atomic reconstructions showed that the regulatory domain was in different orientation in the absence (Rayment et al., 1993) and in the presence (Dominguez et al., 1998) of nucleotide. The velocity of in vitro motion was correlated with the length of the regulatory domain of various myosins (Uyeda et al., 1996; Warshaw et al., 2000). The direction of the rotation of the regulatory domain was correlated with the direction of movement of S1 on actin (Wells et al., 1999). Recent measurements reported a large, ~70° nucleotide-dependent angle change of the light-chain binding region (Shih et al., 2000). Thus, the general consensus has emerged that force production during muscle contraction is caused by the axial rotation of the regulatory domain (Cooke, 1997; Goldman, 1998).

It is not clear, however, whether the regulatory domain rotates as a rigid body, i.e., whether the angular "swing" of the distal end (containing regulatory light chain, RLC) is equal to the swing of the proximal end (containing light chain 1, LC1). The proximal end may be immobilized by the interactions of LC1 with actin and myosin. The N-terminus of LC1 is highly charged and is known to bind to actin (Prince et al., 1981; Sutoh, 1982; Yamamoto and Sekine, 1983; Timson et al., 1998; Andreev and Borejdo, 1995; Andreev et al., 1999) and to myosin heavy chain (Pliszka et al., 2001). At the same time, the C terminus binds to loop 2 of heavy chain, presumably by a mechanism in which the glutamic acid-rich G helix on LC1 binds to the lysine-rich junction between 25 and 50 KDa proteolytic fragments of the catalytic domain (Borejdo et al., 2001).

To test whether the two ends of the regulatory domain rotate differently, we compared the extent and kinetics of the angular motion of the proximal and distal ends. LC1 and RLC were labeled with red and green fluorescent probes, respectively. Fluorescent light chains were exchanged with the native light chains of muscle myosin under the conditions that do not affect muscle function (Borejdo et al., 2001; Irving et al., 1995; Allen et al., 1996; Sabido-David et al., 1998b). The extent and kinetics of transition from rigor

*Submitted October 24, 2001, and accepted for publication February 11, 2002.*

Address reprint requests to Julian Borejdo, Department of Molecular Biology and Immunology, University of North Texas, 3500 Camp Bowie Blvd., Fort Worth, TX 76107-2699. Tel.: 817-735-2106; Fax: 817-735-2133; E-mail: jborejdo@hsc.unt.edu.



0006-3495/02/06/3150/10 $2.00

**TABLE 1 Composition of solutions**

| Solution | $MgCl_2$ | $CaCl_2$ | EGTA | EDTA | ATP |
|---|---|---|---|---|---|
| EGTA-rigor | 4 | | 2 | | |
| EDTA-rigor | | | | 2 | |
| $Ca^{2+}$-rigor | | 0.1 | | | |
| Relaxing | 4 | | 2 | | 4 |
| Glycerinating | 2 | | 5 | | 2 |

All solutions contained 50 mM KCl, 4 mM $MgCl_2$, 10 mM Tris-HCl buffer, pH 7.5. Concentrations are in millimolars.

to relaxation was measured by polarized fluorescence after photogeneration of ATP.

An attempt has been made in this work to minimize the number of observed cross-bridges. Changes of anisotropy are averages over a whole population of observed cross-bridges. Among this population, many cross-bridges do not contribute to force production at all. A significant fraction is weakly bound to actin and is therefore presumably disordered (Cooke et al., 1982; Berger and Thomas, 1993). The strongly bound, ordered force-generating population constitutes only 20% to 29% of the total number (Hopkins et al., 1998; Cooper et al., 2000) and the cross-bridges are distributed between different mechanical states (Eisenberg et al., 1980). Ideally, the anisotropy of a single cross-bridge should be recorded. This has proven impossible so far (the concentration of myosin in fibers is too great), but an attempt is made here to minimize the number of observed cross-bridges by measuring anisotropy by a confocal microscope. Confocal aperture selected a small volume of muscle, containing ~600 fluorescent cross-bridges. ATP was rapidly photogenerated only in this volume. The magnitude of the angular change associated with the transition from rigor to relaxation was similar for both light chains and amounted to less than 5°. The time course of angular change was also similar and consisted of a fast and a slow phase. These results suggest that interactions of LC1 with actin and myosin heavy chain do not inhibit rotation of the proximal end of the regulatory domain and that during contraction the whole domain rotates as a rigid body.

## MATERIALS AND METHODS

### Chemicals and solutions

Standard chemicals, nucleotides, and luciferin-luciferase were from Sigma (St Louis, MO). 5′-iodoacetamidofluorescein (5′-IAF), Alexa Fluor 488 C5 maleimide, and 5-dimethyoxy-2-nitrobenzyl-caged ATP (DMNPE-caged ATP) were from Molecular Probes (Eugene, OR). Composition of solutions are given in Table 1. All solutions used in photolysis experiments contained 10 mM-reduced glutathione. Glycerinating solution contained 80 mM K-acetate, 0.2 mg/mL phenylmethylsulfonyl fluoride, 2 mM $\beta$-mercaptoethanol, and 50% glycerol.

### Preparation of regulatory light chains

RLC containing single cysteine at position 73 (Sabido-David et al., 1998b) was prepared by expressing pT7–7(RLC) construct in BL21(DE3)pLysS cells. The construct was a gift from Dr. S. Lowey (University of Vermont). One-liter cultures were grown for 16 to 18 h at 37°C in an enriched media containing 2% bactotryptone, 1% yeast extract, 0.5% glycerol, 50 mM K-phosphate, pH 7.2, 100 $\mu$g/mL ampicillin, 20 $\mu$g/mL chloramphenicol. Cells were collected at 8000 × $g$ for 10 min, and the RLC was isolated as in Wolff-Long et al. (1993).

### Preparation of essential light chains

The pQE60 vector and *Escherichia coli* M15[pREP4] cells (Qiagen USA, Valencia, CA) were used for the cloning and expression of the essential light chain 1 (LC1). The essential light chain of human fast skeletal muscle essential light chain was subcloned into the pQE60 vector using DNA polymerase chain reaction with the 3′-primer containing a tag of six histidines. The presence of the His-tag at the C terminus of light chain was confirmed by DNA sequencing. The expressed recombinant proteins were purified on the Ni-NTA-agarose columns (Qiagen USA).

### Preparation of muscle fibers

Isolated muscle fibers were prepared from glycerinated rabbit psoas muscle bundles by dissecting single fibers in glycerinating solution and attaching ends of the tautly stretched fiber to the aluminum clips mounted on the microscope slide. Mounted fibers were thoroughly washed with rigor solution and covered with a coverslip.

### Labeling of light chains

The isolated RLC was incubated with 5 M excess of Alexa-Fluor 488 C5 for 24 h in 50 mM KCl, 10 mM phosphate buffer, pH 7.0 (buffer A) at a room temperature. Free dye was removed by Sephadex 50 column followed by dialysis against rigor solution. To prevent aggregation, RLC was stored in a solution containing 10 mM dithiothreitol and 6 M guanidine hydrochloride (Sabido-David et al., 1998b). Before labeling, this solution was replaced by dialysis against buffer A. The degree of labeling was typically 10%. The isolated LC1 was labeled by incubation with 5 M excess of 5′-IATR for 4 h in 50 mM KCl, 10 mM phosphate buffer, pH 7.0 at 4°C. Free dye was removed by Sephadex 50 column followed by dialysis against relaxing solution. The degree of labeling was typically 30%.

### Exchange of RLC into fibers

The labeled RLC was exchanged into fibers as in Ling et al. (1996). The degree of labeling was estimated by comparing the intensity of fluorescence of fibers that underwent exchange with the intensity of known concentration of labeled light chains. Concentration of myosin in the fibers was taken as 120 $\mu$M (Bagshaw, 1982). Approximately 3% of cross-bridges were labeled. Confocal microscope had no trouble detecting such lightly labeled fibers.

### Exchange of LC1 into fibers

The labeled LC1 was exchanged with endogenous light chains of myosin in muscle fibers at 30°C using the exchange solution described by Sweeney (1995). The concentration of trifluoroperazine was decreased to 100 $\mu$M to reduce direct effects of trifluoroperazine on LC1 (Huang et al., 1998) and on RLC (Malmqvist et al., 1997). No CDTA was used. After washing with EDTA-rigor, fibers did not contract in relaxing solution, suggesting that the exchange procedure resulted in only limited extraction of the regulatory proteins. For this reason, the fibers were not irrigated with troponin C. Approximately 5% of cross-bridges were labeled with LC1. Fibers were double labeled by carrying out the exchange with LC1 first.

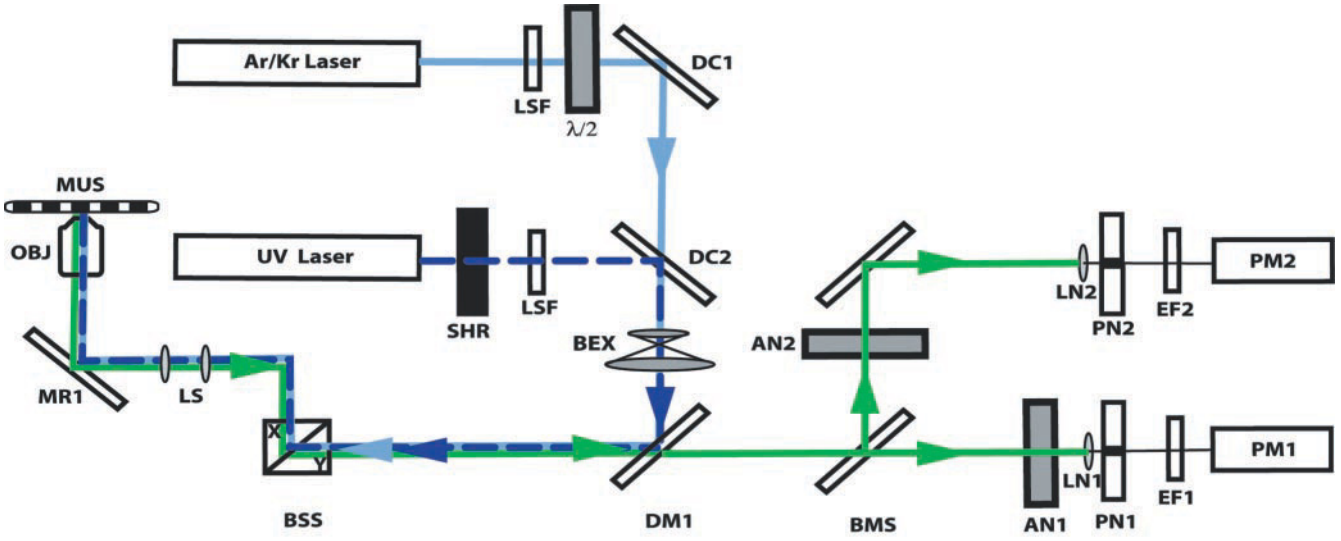


FIGURE 1 Modifications to Zeiss LSM 410 confocal microscope for transient measurements of anisotropy. See text for details. LSF, Light selection fillter; λ/2, mica retarder; DC1 and 2, dichroic combiners; SHR, mechanical shutter; BEX, beam expander; DM1, dichroic mirror; BSS, beam scan system; LS, projection lenses; MR1 and 2, mirrors; OBJ, objective; MUS, muscle fiber; BMS, beam splitter; LN1 and 2, lenses; PN1 and 2, confocal pinholes; AN1 and 2, analyzers; EF1 and 2, emission filters; PM1 and 2, photomultipliers.

## Functionality of exchanged fibers

The effect of exchange on tension development of fibers exchanged with mutant of skeletal RLC labeled at Cys-73 (Sabido-David et al., 1998b) was shown to be negligible. The effect on tension of fibers exchanged with LC1 was measured earlier (Borejdo et al., 2001) and found to be insignificant.

## Specificity of labeling

The specificity of labeling was assessed by inspecting the striation pattern of muscle fibers in a confocal microscope. To maximize the resolution and reduce the thickness of the section, the diameter of the confocal pinhole was minimized (26.3 $\mu$m, 0.65 $\mu$m on image plane). For LC1 and RLC, the average fluorescence of the A bands was three and two times higher than the average fluorescence of the I bands, respectively.

## Experimental arrangement

Zeiss LSM 410 confocal microscope (Zeiss, Thornwood, NY) is modified for anisotropy measurements as follows (Fig. 1). Linearily polarized light from the Ar/Kr laser (Ar/Kr, Series 34, Omnichrome, Chino, CA) operating at 488 or 568 nm (light blue line) is passed through the line selection filter to select desired wavelength. Half-wave plate (λ/2 mica retarder, model WRM 021, Melles Griot, Irvine, CA) sets the direction of excitation polarization. The dichroic combiner 1 projects the beam onto second combiner DC2, which merges visible and ultraviolet (UV) beams. The UV beam, provided by the argon laser (Enterprise, Coherent, Palo Alto, CA) operating at 364 nm (dark blue dashed line), is used to photolyze caged nucleotide. The mechanical shutter SHR (Vincent Associates, Uniblitz T132, Rochester, NY) shuts and opens the UV beam. The beam expander enlarges the combined beams and projects them onto the dichroic mirror 1 and beam scan system. Lenses LS, mirror MR1, and the objective project the scanned beam onto a muscle fiber muscle fiber mounted on the stage of the Axiovert 135 microscope. The emitted light (green) is collected by the objective and is projected onto the beam splitter beam splitter, which passes 50% of emitted light through the first analyzer (AN1) and lens 1 to the confocal pinhole (PN1). The direction of polarization of AN1 can be set to be either perpendicular ($\perp$) or parallel ($\parallel$) to fiber axis. The light then passes through emission filter (EF1) to photomultiplier 1 (PM1). The remaining 50% of the emitted light is passed to the fixed analyzer 2. It is either parallel (if a fiber is horizontal on the stage of a microscope) or perpendicular (when a fiber is vertical) to a fiber axis. The mirror MR2 projects light onto lens 2, confocal pinhole (PN2), the second set of emission filters (EF2) and photomultiplier PM2.

## Measurements of steady-state anisotropy

An axis of a muscle fiber is either vertical or horizontal with respect to the microscope stage. Low aperture lens (10×, NA = 0.22) is used. The exciting wavelength is set at 488 nm for RLC and at 568 for LC1. The half-wave plate is adjusted to polarize the exciting light in the direction perpendicular ($\perp$) or parallel ($\parallel$) with respect to an axis of a fiber. Fluorescence emission is collected in channels 1 and 2, which have the same barrier filters (BP 515–565 nm for RLC and LP $>$ 590 nm for LC1). The sensitivity of photomultiplers is set to optimal. The two fluorescence channels are visualized simultaneously. With fiber axis $\perp$ on the microscope stage, the control measurements are done by setting AN1 to $\perp$. In this case, both emission channels record $\perp$ intensity and should be equal. In practice, they are not equal, due to the fact that the dichroic mirrors and prisms transmit $\parallel$ and $\perp$ light with different efficiencies and due to the differences in the sensitivity of photomultipliers. The intensity ratio PM1/PM2 is the correction factor and varies between 0.40 and 1.90, depending on the exciting wavelength and polarization. The correction factor with a fiber vertical is $C_{\perp}$. With fiber $\parallel$, the control measurements are done by setting AN1 to $\parallel$. The correction factor is $C\parallel$. After making the correction, the actual measurements are taken by setting AN1 to $\parallel$ (with fiber $\perp$) or to $\perp$ (with fiber $\parallel$). Because the correction is done for each area of a fiber separately and because the measurements of $\perp$ and $\parallel$ are made simultaneously, the variations due to fiber inhomogeneity and light variations are minimized. Let the subscript before the measured intensity denote the direction of polarization of incident beam relative to fiber axis, and

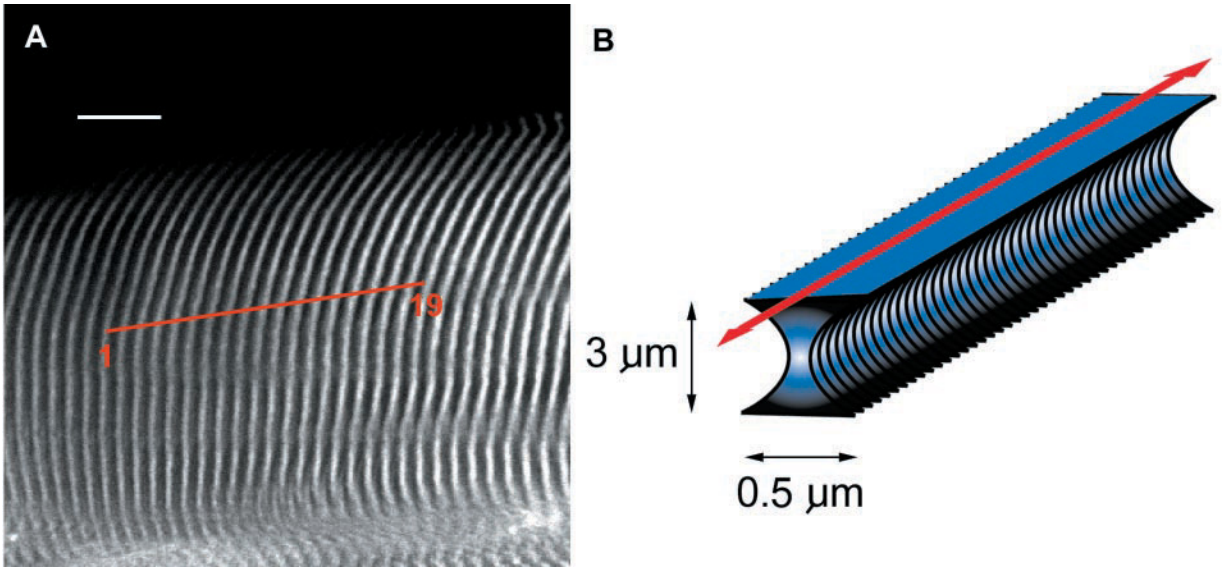


FIGURE 2 Scanning of a muscle fiber. A: Fiber after exchange of LC1. 40 $\mu$m-long line (shown in red) is scanned every 1.394 msec. Line is parallel to fiber axis. Bar is 10 $\mu$m. $\lambda_{ex}$ = 568 nm, $\lambda_{em}$ > 590 nm, sarcomere length 2.22 $\mu$m; B: The cross-section of the laser beam. Drawing not to scale.

subscript after the intensity indicate the direction of polarization of emitted beam. Steady-state anisotropies are:

$$R_\perp = ({}_\perp I_\perp/C_\perp - {}_\perp I_\parallel)/({}_\perp I_\perp/C_\perp + 2\,{}_\perp I_\parallel) \quad (1)$$

$$R_\parallel = ({}_\parallel I_\parallel/C_\parallel - {}_\parallel I_\perp)/({}_\parallel I_\parallel/C_\parallel + 2\,{}_\parallel I_\perp) \quad (2)$$

The two images of fiber are stored on the computer disk. The intensities recorded by PM1 and PM2 are measured from the same region of interest of both images by Image Plus (Media Cybernetics, Silver Spring, MD).

## Measurements of transient anisotropy

High aperture lens (C-Apo, 40×, NA = 1.2) is used. To avoid photobleaching, laser beam is allowed to dwell on a spot only for 6.4 $\mu$s. After 6.4 $\mu$s, it is moved along a line by 0.46 or by 0.18 $\mu$m and the process is repeated 218 times. As a result a laser spot is scanned along either $L$ = 100 or $L$ = 40 $\mu$m line. Fig. 2 illustrates how the measurements are done. Scan line is drawn in red. Scan begins at time 0. At this time sarcomere 1 is being illuminated with a sampling beam (488 or 568 nm). Its size is ~0.5 $\mu$m × 0.5 $\mu$m. It has a Gaussian shape (Fig. 2 *B*). The last sarcomere along a line (19 in this case) is always illuminated 218 × 6.4 $\mu$s = 1.394 ms after the first one. Scanning galvanometers move in a harmonic fashion, i.e., a line is scanned 218 times (in 1.394 ms) regardless of its length. (In Zeiss LSM 410 a line is always sampled 218 times. There is no way to decrease it and improve the time resolution.) During one 1.394-ms-long sweep of a line, video card (Matrox Imaging Series) calculates "anisotropy" functions:

$$R_\perp(t) = [({}_\perp I_\perp(t) - {}_\perp I_\parallel(t))/({}_\perp I_\perp(t) + 2\,{}_\perp I_\parallel(t))] \times 256 + 128 \quad (3)$$

$$R_\parallel(t) = [({}_\parallel I_\perp(t) - {}_\parallel I_\parallel(t))/({}_\parallel I_\parallel(t) + 2\,{}_\parallel I_\parallel(t))] \times 256 + 128 \quad (4)$$

in which ${}_\perp I_\perp(t)$, ${}_\perp I_\parallel(t)$, ${}_\parallel I_\perp(t)$, and ${}_\parallel I_\parallel(t)$ are the instantaneous fluorescence intensities at time $t$. $R$ values are not the time-resolved anisotropies but changes in steady-state anisotropies. During the first sweep, video card calculates mean of 218 numbers, which corresponds to the anisotropy at time $t_0$. A line is swept again 1.394 ms later with a mean corresponding to the anisotropy at time $t_1$ = 1.394 ms. The process is repeated 512 times with the last seep giving anisotropy at time $t_{512}$ = 713.7 ms.

## Photogeneration of ATP

A shutter inserted after the exit aperture of the UV laser is opened briefly to expose muscle to the UV light. Muscle is perfused with 2 mM of 5-dimethyoxy-2-nitrobenzyl-caged ATP (DMNPE-caged ATP). The UV beam is focused by the objective to a Gaussian spot with the width and length equal to twice the lateral resolution of the UV beam (~0.2 $\mu$m), and the height equal to the depth of focus of the objective (~3 $\mu$m). The beam dwells on this spot for 6.4 $\mu$s, during which time enough energy is supplied to the muscle to convert all caged ATP into ATP (see below). After 6.4 $\mu$s, the laser beam is moved along the red line (Fig. 2) to the next spot. The process is repeated until the last spot in a line is illuminated. As a consequence, each spot remains in the dark for 1.394 ms. Yet during each scan, the level of ATP along chosen line is maintained at the approximately constant level because ATP diffuses away within ~1 ms (Hubley et al., 1996). An advantage of the present method of uncaging is that ATP within muscle is constantly regenerated offsetting depletion due to ATP hydrolysis. The disadvantage is that in muscle diffusion may be slowed down by obstacles (Saxton, 1994), making it impossible to determine the exact concentration of ATP in the observed volume.

The laser provides 16 mW = 16 mJ/s of continuous power. Only 0.12 mJ/s is incident on the muscle, because of the clipping of the enlarged laser beam by the entrance aperture of the objective, loss at the dichroic mirror 1, and loss due to absorption by glass in the objective. The area illuminated by UV is $(0.04)^2$ $\mu$m$^2$. The energy flux at the illuminated area is 0.12 mJ/(s × $0.04^2$ $\mu$m$^2$) = 3.0 mJ/(s × $\mu$m$^2$). The dwell time of the laser beam is 6.4 $\mu$s. The energy flux through the illuminated area during a dwell time is 2 × $10^{-5}$ mJ. This is similar to the energy flux obtainable with frequency-doubled ruby laser (~3 × $10^{-5}$ mJ/$\mu$m$^2$) (Goldman et al., 1984).

**TABLE 2 Steady-state polarizations of muscle containing LC1-IATR and RLC-Alexa488**

| State | Light chain | Label | $\lambda_{exc}$ (nm) | $P_{\parallel} \pm$ SEM | $P_{\perp} \pm$ SEM | $N$ | $\Theta_o$ (deg) | $\delta$ (deg) |
|---|---|---|---|---|---|---|---|---|
| Rigor | RLC | Alexa488 | 488 | 0.189 ± 0.018 | 0.269 ± 0.007 | 5 | 52 | 25 |
| Relax | RLC | Alexa488 | 488 | 0.284 ± 0.007 | 0.252 ± 0.022 | 5 | 49 | 25 |
| Rigor | LC1 | Rhodamine | 568 | 0.373 ± 0.023 | 0.298 ± 0.007 | 5 | 47 | 20 |
| Relax | LC1 | Rhodamine | 568 | 0.336 ± 0.009 | 0.347 ± 0.006 | 5 | 52 | 19 |

To facilitate comparison with other work, the values are given as polarizations (using the formula relating anisotropy $R$ to polarization $P$ ($R = 2P/(3 - P)$).

## Estimating the amount of ATP photoreleased during a scan

The amount of ATP produced in a single experiment was estimated by measuring the luminescence of luciferin-luciferase (LL) solution exposed to the UV beam. Ten microliters of rigor solution containing 2 mM caged ATP were illuminated by 0.12 mW UV beam for 1, 30, and 60 s. Five microliters of 40 mg/mL of LL was placed on x-ray film (Kodak, Rochester, NY) and mixed with 5 $\mu$L of solution containing photogenerated ATP. The film was exposed for 10 min. The calibration curve was obtained by mixing known amounts of ATP with LL solution. The film was scanned by MicroTek ScanMaker 4 scanner. Optical density was measured by Image Plus Pro (Media Cybernetics, Silver Spring, MD). During 1-s exposure, $10^{-12}$ mol of ATP were produced. Therefore, during one dwell time, $6.4 \times 10^{-18}$ mol are produced. Assuming that the volume illuminated by the UV light is $10^{-15}$ L, the flux of UV light is sufficient to generate $6.4 \times 10^{-18}/(10^{-15}) = 6.4$ mM ATP. This is more than the concentration of applied precursor. We conclude that all caged ATP is converted into ATP. As mentioned before, the actual concentration of ATP within the experimental volume is not known, but it is greater than the concentration of the precursor.

The concentration of ATP in muscle chamber released during each experiment is exceedingly small—not enough to cause whole muscle to contract. $10^{-13}$ mol ATP is released during 100 ms. The volume of experimental trough is $2 \times 10^{-5}$ L, so the concentration of ATP accumulated during one experiment is $10^{-5}$ mM.

## Number of observed cross-bridges

The objective (40×, NA = 1.2), illumination wavelength (488 or 568 nm), and the size of the confocal aperture (35 $\mu$m) define the observed volume at ~0.3 $\mu$m$^3$. The concentration of myosin in muscle is 120 $\mu$M (Bagshaw, 1982), giving $2.1 \times 10^4$ myosin molecules in the observed volume. Because only 3% to 5% of cross-bridges contain labeled light chain, ~600 cross-bridges contribute to the observed signal.

## Estimating the amount of heat generated in the illuminated volume

Laser energy is absorbed principally by caged-ATP. Laser delivers 0.12 mJ/s, i.e., $0.8 \times 10^{-9}$ J in one dwell time. Extinction coefficient of caged-ATP at 364 nm is 4400 M$^{-1}$ cm$^{-1}$. The energy absorbed by muscle during one dwell time is $0.8 \times 10^{-12}$ J. Because it takes $4.2 \times 10^{-12}$ J to heat up the experimental volume by 1°C, the temperature rise during an experiment is less than 1/20°C. The increase in temperature caused by the absorption by Alexa and rhodamine is at least six times smaller (concentration of dye is 100 times smaller, absorption coefficient is 16 times larger).

# RESULTS

## Steady-state polarization

Table 2 summarizes polarizations in rigor and relaxation. For RLC in rigor, $P_{\perp} > P_{\parallel}$ suggesting that the dipoles are preferentially oriented in a direction perpendicular to the fiber axis. The opposite is true for LC1 in rigor. There was no statistically significant difference between P values in relaxation. This suggests that the cross-bridges are disordered. These data were fitted by a Gaussian model of distribution of cross-bridges (Thomas and Cooke, 1980; Wilson and Mendelson, 1983). In this model, $\Theta$, the polar angle that the dipoles make with the vertical, and the standard deviation ($\delta$) with which the dipoles are distributed around the mean value $\Theta_o$ have Gaussian probability $r(\Theta) = \exp[-(\Theta - \Theta_o)^2/2\delta^2]$. The angles were estimated by the method of Xiao et al. (1995). The values for the orientation of probes on RLC were 52 ± 25° and 49 ± 25° in rigor and relaxation, respectively. The errors are larger than reported by Allen et al. (1996), Sabido-David et al. (1998a,b), and Hopkins et al. (1998). The values for the orientation of probes on LC1 were 47 ± 20° and 52 ± 19° in rigor and relaxation, respectively. The modest size of rotation is consistent with earlier work (Allen et al., 1996; Hopkins et al., 1998; Sabido-David et al., 1998).

## Anisotropy change of RLC during photorelease of ATP

Fiber is exchanged with fluorescent light chain, placed vertically on a microscope stage, perfused with caged ATP, and illuminated with visible light, which is polarized $\perp$ or $\parallel$ to muscle axis. Diffraction limited laser spot is scanned along $L = 40$ $\mu$m or $L = 100$ $\mu$m line to minimize photobleaching. The experiment is begun by initiating the scan and opening the shutter admitting the UV light. Shutter remains open for exactly 100 ms, after which the muscle reverts to being illuminated with the sampling beam only. The process is repeated 512 times. Fig. 3 *A* shows a typical example of a time course of change of perpendicular anisotropy of muscle exchanged with RLC (the anisotropy $R$ is related to the polarization of fluorescence $P$ by $R = 2P/(3 - P)$). Fig. 3 *B* shows the fit of the decay to a single (solid) and double exponential (dashed) lines. The double exponential fit (green) ($R^2 = 0.938$) was significantly better than a single exponential one (red) ($R^2 = 0.911$). Goodness of fit is reflected in the fact that the residuals (inset) of dashed line fit were significantly smaller at the early times then the residuals of solid line fit. This suggests that the fast process

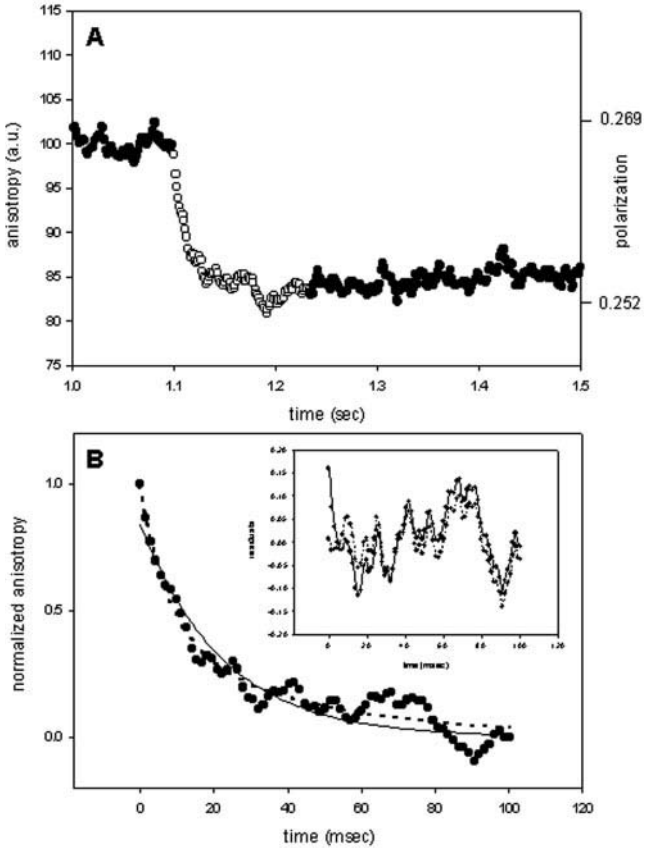


FIGURE 3 (*A*) $R_\perp$ of a fiber containing RLC-labeled with Alexa488. (○) Fiber exposed to the UV. The anisotropy was measured with $\lambda_{ex} = 488$ nm, $515 < \lambda_{em} < 565$ nm, $L = 40$ $\mu$m. (*Right scale*) Absolute change from Table 2. (*B*) Fit to a single (*solid line*) and a double (*dashed line*) exponentials. Single and double exponential fits are $R_\perp = 0.84\ e^{-0.046t}$ and $R_\perp = 0.58\ e^{-0.130t} + 0.42\ e^{-0.024t}$. (*Inset*) Residuals of single (*solid line*) and double (*dashed line*) exponential fits. EGTA-rigor, 2 mM caged-ATP.

was followed by the slower one, with a rate constant approximately five times smaller. The average half-time ± SEM of change of fast phase in 12 experiments was 17 ± 8 ms (minimum = 6, maximum = 31 ms, Table 3). These data are in agreement with earlier results of Allen et al. (1996). The absolute change (right axis) was taken from the steady-state results (Table 2). The anisotropy measurements are relative, because *R* functions (Eqs. 3 and 4) are calculated using fluorescent intensities that are not corrected for the background or for the instrumental depolarization. Moreover, to tightly focus UV light to produce high enough

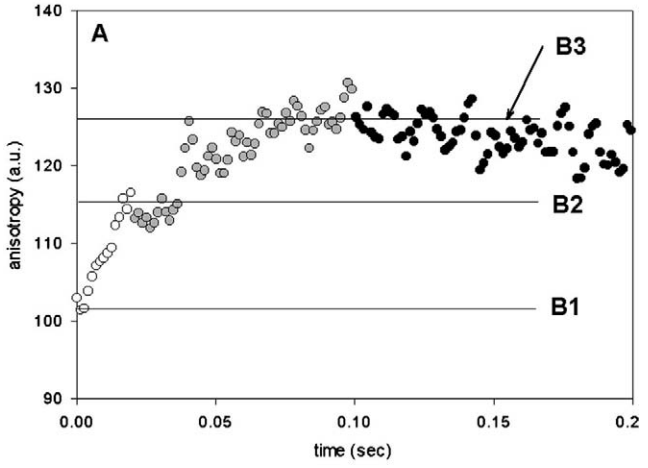


FIGURE 4 The quantification of the anisotropy change. Fast (*white circles*) and slow (*gray circles*) phases were fitted to straight lines (in this case with half-times of 16 and 45 ms). (*Black circles*) Fiber is not exposed to the UV. $R_\perp$, $\lambda_{ex} = 568$ nm, $\lambda_{em} > 590$ nm, $L = 40$ $\mu$m. Fiber exchanged with LC1–5′-IATR. EGTA-rigor, 2 mM caged-ATP.

flux to photogenerate ATP, the measurements have to be done with high NA objective. This produces additional depolarization (Axelrod, 1979).

## Anisotropy change of LC1 during photorelease of ATP

Fig. 4 shows an example of the time course of change of anisotropy of muscle exchanged with LC1. The control experiments carried out on the same fiber in the absence of caged ATP showed no change of anisotropy (not shown). The same line could be sampled repetitively with little difference in the time course (not shown), suggesting that the UV light at 364 nm does not cause damage to muscle. There was no change in the anisotropy during the exposure to the UV light when ADP was produced, but a small increase was sometimes observed after the UV light was turned off (not shown). Parallel and perpendicular anisotropies behaved reciprocally, and the presence of $Ca^{2+}$ made no difference to the time course (Weber and Murray, 1973) (not shown).

Fig. 4 illustrates how the change of the anisotropy was quantified. The rates of fast (open circles) and slow (shaded circles) changes were estimated from a fit to straight lines.

**TABLE 3 Half times and amplitudes of the fast and slow changes in anisotropy**

| Phase, light chain | Half time ± SEM (ms) | Min $\tau$ (ms) | Max $\tau$ (ms) | Normalized amplitude ±SEM | *N* |
|---|---|---|---|---|---|
| Fast, RLC | 17±8 | 6 | 31 | — | 12 |
| Fast, LC1 | 13±4 | 4 | 29 | 1.00 | 46 |
| Slow, LC1 | 35±3 | 17 | 57 | 0.37 ± 0.03 | 26 |

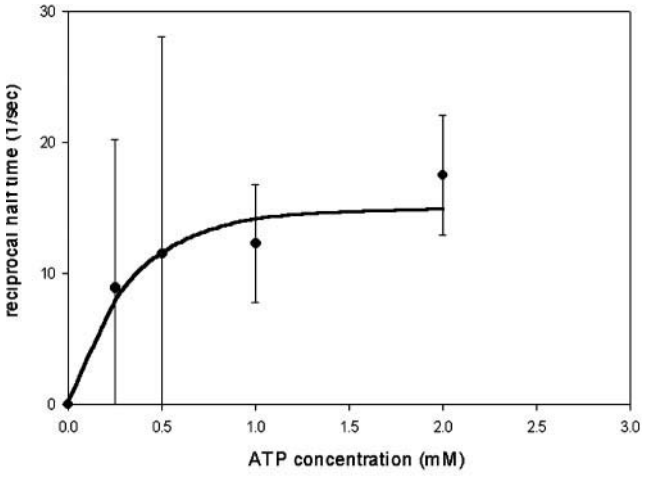


FIGURE 5 Dependence of the half time of the fast phase of anisotropy change on the concentration of ATP. Reciprocal half time is plotted against the concentration of ATP. Errors are the standard deviations of four experiments. UV flux is sufficient to convert all caged precursor to nucleotide. Hence, the concentration of ATP is equal to the concentration of caged ATP applied to the sample. ●, Experimental data; red line, single exponential fit.

The quality of data did not allow differentiation between exponential and linear fits. Rates were expressed as half of the time needed for the anisotropy to change between baselines. Baseline 1 was equal to a level of the anisotropy before turning on the UV. Baseline 2 was equal to the level of the anisotropy at an inflection point between the fast and slow processes. Baseline 3 was equal to the level of the anisotropy after turning off the UV. The rates were dependent on the subjective selection of baselines. The amplitudes of fast and slow processes were B2-B1 and B3-B2, respectively. The amplitude of the slow process constituted $0.37 \pm 0.03$ of the amplitude of the fast process. The results are summarized in Table 3. The rate of change of the fast phase of LC1 and the rate of change of RLC were not significantly different ($t = -2.04$, $p = 0.046$).

The rate of the fast change depended on the concentration of ATP. Fig. 5 shows the plot of the reciprocal half time versus ATP concentration. The second-order rate constant was $k_{obs} = 4 \times 10^4\ M^{-1}s^{-1}$. We think that this process reflects dissociation of myosin heads from actin (see Discussion).

## Double-labeled fibers

To measure the time course of rotations at the same time, fibers were exchanged with fluorescent adducts of both light chains. Even though the probability that both fluorescent light chains reside on the same cross-bridge is remote (more likely ~300 cross-bridges contain only LC1 and ~300 different cross-bridges only RLC), at least the anisotropy is measured from the same small population of cross-bridges. Fig. 6 shows that by choosing appropriate filter combinations, either LC1 (A) or RLC (B) within the same fiber can be visualized. The time courses of change of parallel anisotropy of LC1 and RLC are shown in Fig. 7. The most prominent feature of the curves is that the time courses are similar. This is more clearly illustrated in Fig. 8, which shows time correlation between parallel (A) and perpendicular (B) anisotropies.

## DISCUSSION

The values of polarizations of RLC and LC1 (Table 2) indicated that the absolute magnitude of motion of the proximal and distal parts of the regulatory domain were the same upon transition from rigor to relaxation. Likewise, the rates of the fast phases of the rotary motion of RLC and LC1 reflecting transition from rigor to relaxation (Table 3) were

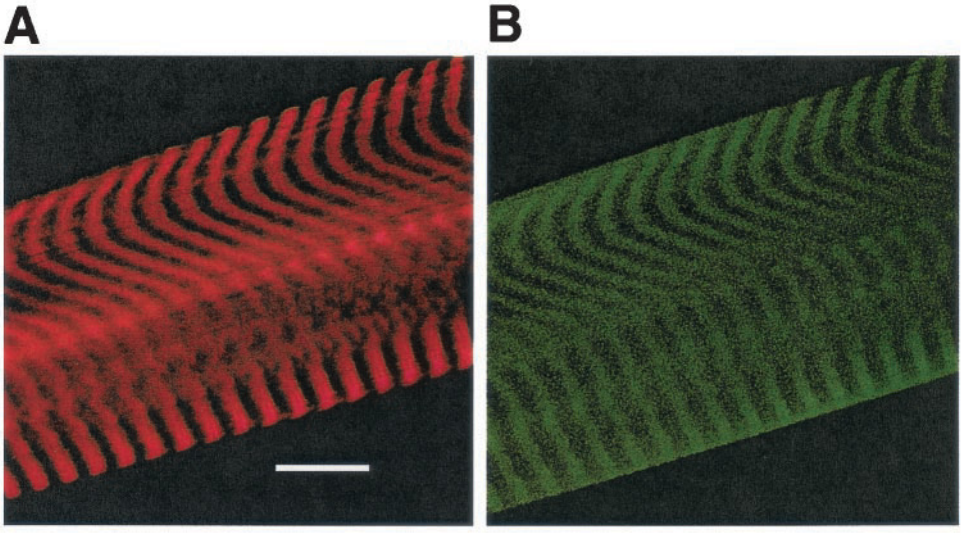


FIGURE 6 Muscle fiber exchanged with fluorescent LC1 (*A*) ($\lambda_{ex} = 568$ nm, $\lambda_{em} > 590$ nm) and RLC (B) ($\lambda_{ex} = 488$ nm, $515 < \lambda_{em} < 565$ nm). Diameter of confocal pinhole 0.656 $\mu$m on image plane; thickness of section, 1.03 $\mu$m; bar, 10 $\mu$m; sarcomere length, 3.26 $\mu$m.

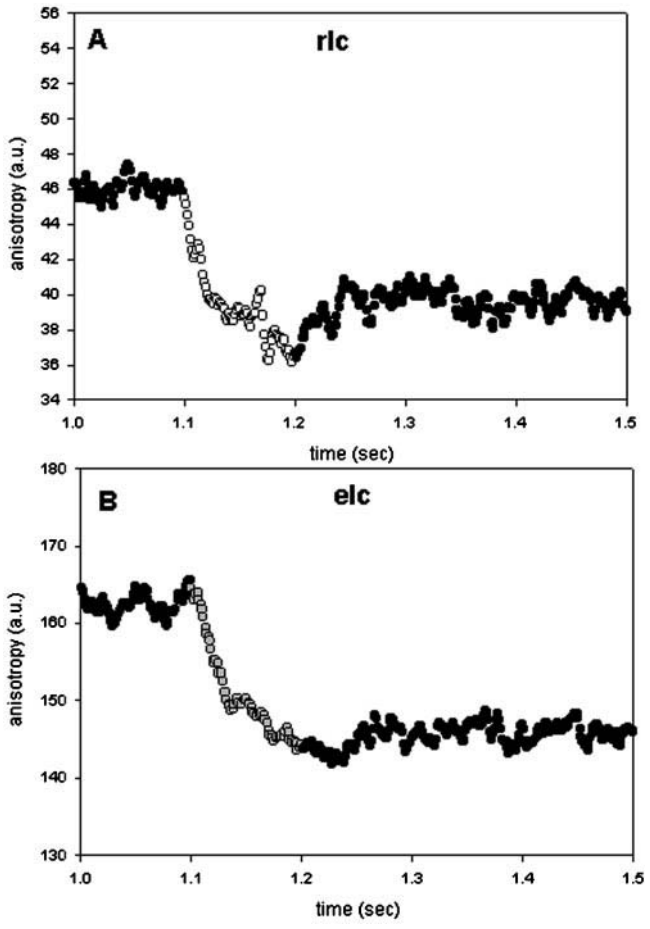


FIGURE 7 Transient change of $R\|$. Fiber exchanged with both LC1 and RLC. (*Open* and *shaded circles*) Fiber exposed to the UV. (*A*) $R_\|$ of RLC, $\lambda_{ex} = 488$ nm, $515 < \lambda_{em} < 565$ nm, $L = 40$ $\mu$m. To facilitate comparison, the direction of change has been reversed. (*B*) $R_\|$ of LC1, $\lambda_{ex} = 568$ nm, $\lambda_{em} > 590$ nm, $L = 40$ $\mu$m. EGTA-rigor, 2 mM caged-ATP.

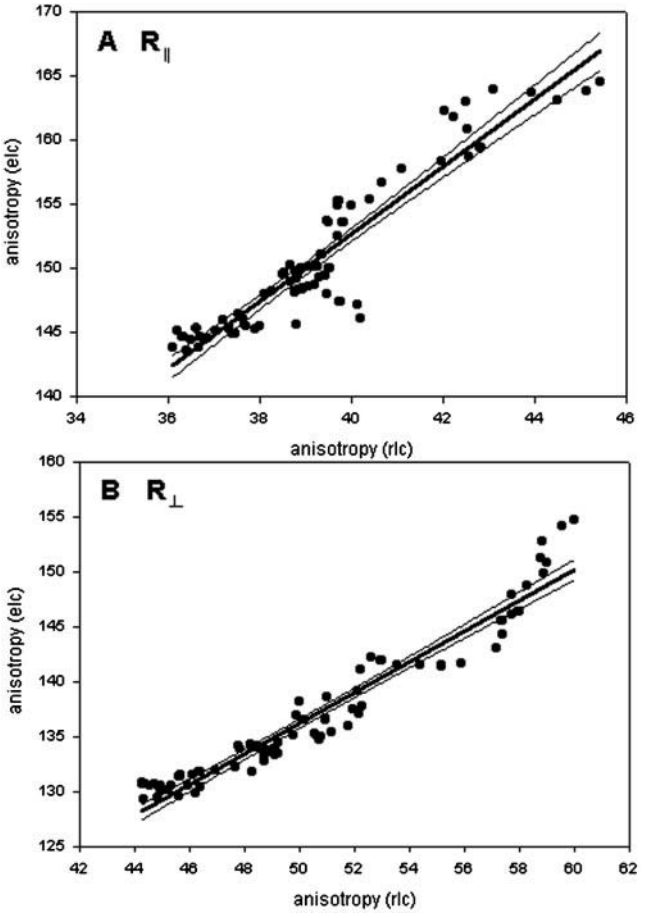


FIGURE 8 The correlation of the time courses of rotations of RLC and LC1. (*A*) Parallel anisotropy, data from Fig. 8; (*B*) perpendicular anisotropy (data not shown). Thick lines are linear regressions; thin lines indicate 95% confidence limits.

statistically the same. We conclude that the two ends of the regulatory domain reflect the same motion.

The experiments involved sudden presentation of ATP to muscle in rigor. This suggests that the rotary motion observed in our experiments reflects dissociation of cross-bridges from thin filaments. The fact that the rate of the fast reorientation depended on concentration of ATP in the second-order manner reinforces this suggestion. The same conclusion was reached earlier by Allen et al. (1996 ). It is unlikely that the anisotropy change reflects any other step in the cross-bridge cycle. Thus, the repriming of cross-bridges that follows dissociation is likely to be fast, because S1 is tethered to thick filaments by the highly flexible S1-S2 joint: Tethered S1 rotates nearly as fast as free S1 (rotational correlation time less than 300 ns (Mendelson et al., 1973; Cheung et al., 1991)). Likewise, the reorientation of S1 associated with the power stroke is fast (Huxley and Simmons, 1971; Hopkins et al., 1998). The kinetics of dissociation must be the same regardless of whether the final state of muscle is contraction or relaxation (i.e., whether the initial rigor solution contains $Ca^{2+}$ or not).

The suggestion that the proximal and distal parts of the regulatory domain undergo the same rotary motion upon dissociation from thin filaments is reinforced by the direct comparison of rotation of RLC and LC1 in double-labeled fibers, which also showed good correlation between rotations (Fig. 8). Thus experiments on single- and double-labeled fibers suggest that light chains located at the opposite ends of the regulatory domain rotate similarly and lead us to the conclusion that the domain behaves a rigid body. Thus the interactions LC1 with actin (Prince et al., 1981; Sutoh, 1982; Yamamoto and Sekine, 1983; Timson et al., 1998; Andreev and Borejdo, 1995; Andreev et al., 1999) and with myosin heavy chain (Borejdo et al., 2001; Pliszka et al., 2001) do not influence its mobility.

Our results suggest that the dissociation of cross-bridges is not a simple exponential process. Rather, the fast phase of rotation is followed by a slower one with the average half time nearly three times longer than the fast phase and three

times smaller amplitude (Table 3). Possibly, two steps reflect dissociation of the primary binding site on S1 followed by slower dissociation of the secondary site (Andreev and Borejdo, 1995).

The principal advantage of our method is that it is possible to measure kinetics of a small number of cross-bridges in working muscle. By increasing the sensitivity of a microscope (e.g., replacing photomultipliers with avalanche photodiodes), we should be able to observe ~10 cross-bridges. The sophisticated techniques that have been developed to observe mechanical (Finer et al., 1994; Miyata et al., 1994; Block and Svoboda, 1995; Molloy et al., 1995; Guilford et al., 1997; Warshaw et al., 1998) and chemical (Funatsu et al., 1995; Ishijima et al., 1998) events of a single myosin molecule in vitro cannot be applied to muscle fibers. The concentration of myosin in muscle fiber (120 $\mu$M, (Bagshaw, 1982)) is simply too great. Remarkable advances have been made by studying acto-myosin in vitro (e.g., Finer et al., 1994; Miyata et al., 1994; Block and Svoboda, 1995; Molloy et al., 1995; Funatsu et al., 1995; Guilford et al., 1997; Ishijima et al., 1998; Warshaw et al., 1998; Suzuki et al., 1998), but to gain complete understanding of the mechanism of muscle action, it is necessary to observe few molecules of myosin during a contraction of a muscle fiber.

Other advantages of our method are that the same cross-bridges can be sampled repetitively, that photogenerating ATP continuously offsets depletion of ATP by hydrolysis, that the degree of synchronization induced by a sudden appearance of ATP within small volume is high (J. Borejdo and I. Akopova, unpublished data), that the amount of caged compound used is minimal, and that movement artifacts are eliminated (our fibers do not generate tension because the amount of ATP photogenerated locally is not enough to induce contraction of a whole fiber). The principal disadvantage is that only the relative anisotropy can be measured. It is possible to calibrate anisotropy curves by using the steady-state data (Fig. 3), but it is only an indirect estimate. Other disadvantages are that the final concentration of ATP is unknown (problem which will be fixed with the use of 2-photon excitation) and that it is not possible to measure force and anisotropy at the same time.

## REFERENCES


Allen, T. S.-C., N. Ling, M. Irving, and Y. E. Goldman. 1996. Orientation changes in myosin regulatory light chains following photorelease of ATP in skinned muscle fibers. *Biophys. J.* 70:1847–1862.

Andreev, O. A., and J. Borejdo. 1995. Binding of heavy- and essential light-chain 1 of S1 to actin depends on the degree of saturation of F-actin filaments with S1. *Biochemistry.* 34:14829–14833.

Andreev, O. A., L. D. Saraswat, S. Lowey, C. Slaughter, and J. Borejdo. 1999. Interaction of the N-terminus of chicken skeletal essential light chain 1 with F-actin. *Biochemistry.* 38:2480–2485.

Axelrod, D. 1979. Carbocyanine dye orientation in red cell membrane studied by microscopic fluorescence polarization. *Biophys. J.* 26: 557–573.

Bagshaw, C. R. 1982. Muscle Contraction. Chapman and Hall, London.

Berger, C. L., and D. D. Thomas. 1993. Rotational dynamics of actin-bound myosin heads in active myofibril. *Biochemistry.* 32:3812–3821.

Block, S. M., and K. Svoboda. 1995. Analysis of high-resolution recordings of motor movement. *Biophys. J.* 68:2305S–2395S.

Borejdo, J., D. Ushakov, R. Moreland, I. Akopova, Y. Reshetnyak, L. D. Saraswat, K. Kamm, and S. Lowey. 2001. The power stroke causes changes in orientation and mobility of the termini of essential light chain 1 of myosin. *Biochemistry.* 40:3796–3803.

Burghardt, T. P., S. P. Garamszegi, S. Park, and K. Ajtai. 1998. Tertiary structural changes in the cleft containing the ATP sensitive tryptophan and reactive thiol are consistent with pivoting of the myosin heavy chain at Gly699. *Biochemistry.* 37:8035–8047.

Cheung, H. C., I. Gryczynski, H. Malak, W. Wiczk, M. L. Johnson, and J. R. Lakowicz. 1991. Conformational flexibility of the Cys-697-Cys-707 segment of myosin subfragment-1: distance distributions by frequency-domain fluorometry. *Biophys. Chem.* 40:1–17.

Cooke, R. 1997. Actomyosin interaction in striated muscle. *Physiol. Rev.* 77:671–697.

Cooke, R., M. S. Crowder, and D. D. Thomas. 1982. Orientation of spin labels attached to cross-bridges in contracting muscle fibres. *Nature.* 300:776–778.

Cooper, W. C., L. R. Chrin, and C. L. Berger. 2000. Detection of fluorescently labeled actin-bound cross-bridges in actively contracting myofibrils. *Biophys. J.* 78:1449–1457.

Corrie, J. E., B. D. Brandmeier, R. E. Ferguson, D. R. Trentham, J. Kendrick-Jones, S. C. Hopkins, U. A. van der Heide, Y. E. Goldman, C. Sabido-David, R. E. Dale, S. Criddle, and M. Irving. 1999. Dynamic measurement of myosin light-chain-domain tilt and twist in muscle contraction. *Nature.* 400:425–430.

Dominguez, R., Y. Freyzon, K. M. Trybus, and C. Cohen. 1998. Crystal structure of a vertebrate smooth muscle myosin motor domain and its complex with the essential light chain: visualization of the pre-power stroke state. *Cell.* 94:559–571.

Eisenberg, E., T. L. Hill, and Y. Chen. 1980. Cross-bridge model of muscle contraction: quantitative analysis. *Biophys. J.* 29:195–227.

Finer, J. T., R. M. Simmons, and J. A. Spudich. 1994. Single myosin molecule mechanics: piconewton forces and nanometre steps. *Nature.* 368:113–119.

Funatsu, T., Y. Harada, M. Tokunaga, K. Saito, and T. Yanagida. 1995. Imaging of single fluorescent molecules and individual ATP turnovers by single myosin molecules in aqueous solution. *Nature.* 374:555–559.

Goldman, Y. E. 1998. Wag the tail: structural dynamics of actomyosin. *Cell.* 93:1–4.

Goldman, Y. E., M. G. Hibberd, and D. R. Trentham. 1984. Relaxation of rabbit psoas muscle fibres from rigor by photochemical generation of adenosine-5′-triphosphate. *J. Physiol. (Lond).* 354:577–604.

Guilford, W. H., D. E. Dupuis, G. Kennedy, J. Wu, J. B. Patlak, and D. M. Warshaw. 1997. Smooth muscle and skeletal muscle myosins produce similar unitary forces and displacements in the laser trap. *Biophys. J.* 72:1006–1021.

Hopkins, S. C., C. Sabido-David, J. E. Corrie, M. Irving, and Y. E. Goldman. 1998. Fluorescence polarization transients from rhodamine isomers on the myosin regulatory light chain in skeletal muscle fibers. *Biophys. J.* 74:3093–3110.

Huang, W., G. J. Wilson, L. J. Brown, H. Lam, and B. D. Hambly. 1998. EPR and CD spectroscopy of fast myosin light chain conformation during binding of trifluoperazine. *Eur. J. Biochem.* 257:457–465.

Hubley, M. J., B. R. Locke, and T. S. Moerland. 1996. The effects of temperature, pH, and magnesium on the diffusion coefficient of ATP in solutions of physiological ionic strength. *Biochim. Biophys. Acta.* 1291: 115–121.

Huxley, A. F., and R. M. Simmons. 1971. Proposed mechanism of force generation in striated muscle. *Nature.* 233:533–538.

Irving, M., T. St Claire Allen, C. Sabido-David, J. S. Craik, B. Brandmeier, J. Kendrick-Jones, J. E. Corrie, D. R. Trentham, and Y. E. Goldman. 1995. Tilting of the light-chain region of myosin during step length changes and active force generation in skeletal muscle. *Nature.* 375: 688–691.

Ishijima, A., H. Kojima, T. Funatsu, M. Tokunaga, H. Higuchi, H. Tanaka, and T. Yanagida. 1998. Simultaneous observation of individual ATPase and mechanical events by a single myosin molecule during interaction with actin. *Cell.* 92:161–171.

Ling, N., C. Shrimpton, J. Sleep, J. Kendrick-Jones, and M. Irving. 1996. Fluorescent probes of the orientation of myosin regulatory light chains in relaxed, rigor, and contracting muscle. *Biophys. J.* 70:1836–1846.

Malmqvist, U., K. Trybus, S. Yagi, J. Carmichael, and F. Fay. 1997. Slow cycling of unphosphorylated myosin is inhibited by calponin, thus keeping smooth muscle relaxed. *Proc. Natl. Acad. Sci. U.S.A.* 94:7655–7660.

Mendelson, R., M. F. Morales, and J. Botts. 1973. Segmental flexibility of S1 moiety of myosin. *Biochemistry.* 12:2250–2255.

Miyata, H., H. Hakozaki, H. Yoshikawa, N. Suzuki, K. Kinosita, Jr., T. Nishizaka, and S. Ishiwata. 1994. Stepwise motion of an actin filament over a small number of heavy meromyosin molecules is revealed in an in vitro motility assay. *J. Biochem. (Tokyo).* 115:644–647.

Molloy, J. E., J. E. Burns, J. Kendrick-Jones, R. T. Tregear, and D. C. White. 1995. Movement and force produced by a single myosin head. *Nature.* 378:209–212.

Pliszka, B., M. J. Redowicz, and D. Stepkowski. 2001. Interaction of the N-terminal part of the A1 essential light chain with the myosin heavy chain. *Biochem. Biophys. Res. Commun.* 281:924–928.

Prince, H. P., H. R. Trayer, G. D. Henry, I. P. Trayer, D. C. Dalgarno, B. A. Levine, P. D. Cary, and C. Turner. 1981. Proton nuclear-magnetic-resonance spectroscopy of myosin subfragment 1 isoenzymes. *Eur. J. Biochem.* 121:213–219.

Rayment, I., W. Rypniewski, K. Schmidt-Base, R. Smith, D. R. Tomchik, M. M. Benning, D. A. Winkelman, G. Wesenberg, and H. M. Holden. 1993. Three-dimensional structure of myosin subfragment-1: a molecular motor. *Science.* 261:50–58.

Sabido-David, C., B. Brandmeier, J. S. Craik, J. E. Corrie, D. R. Trentham, and M. Irving. 1998a. Steady-state fluorescence polarization studies of the orientation of myosin regulatory light chains in single skeletal muscle fibers using pure isomers of iodoacetamidotetramethylrhodamine. *Biophys. J.* 74:3083–3092.

Sabido-David, C., S. C. Hopkins, L. D. Saraswat, S. Lowey, Y. E. Goldman, and M. Irving. 1998b. Orientation changes of fluorescent probes at five sites on the myosin regulatory light chain during contraction of single skeletal muscle fibres. *J. Mol. Biol.* 279:387–402.

Saxton, M. J. 1994. Anomalous diffusion due to obstacles: a Monte Carlo study. *Biophys. J.* 66:394–401.

Shih, W. M., Z. Gryczynski, J. R. Lakowicz, and J. A. Spudich. 2000. A FRET-based sensor reveals large ATP hydrolysis-induced conformational changes and three distinct states of the molecular motor myosin. *Cell.* 102:683–694.

Sutoh, K. 1982. Identification of myosin binding sites on the actin sequence. *Biochemistry.* 21:3654–3661.

Suzuki, Y., T. Yasunaga, R. Ohkura, T. Wakabayashi, and K. Sutoh. 1998. Swing of the lever arm of a myosin motor at the isomerization and phosphate-release steps. *Nature.* 396:380–383.

Sweeney, H. L. 1995. Function of the N-terminus of the myosin essential light chain of vertebrate striated muscle. *Biophys. J.* 68:112s–119s.

Thomas, D. D., and R. Cooke. 1980. Orientation of spin-labeled myosin heads in glycerinated muscle fibers. *Biophys. J.* 32:891–905.

Timson, D. J., H. R. Trayer, and I. P. Trayer. 1998. The N-terminus of A1-type myosin essential light chains binds actin and modulates myosin motor function. *Eur. J. Biochem.* 25:654–662.

Uyeda, T. Q., P. D. Abramson, and J. A. Spudich. 1996. The neck region of the myosin motor domain acts as a lever arm to generate movement. *Proc. Natl. Acad. Sci. U.S.A.* 93:4459–4464.

Warshaw, D. M., W. H. Guilford, Y. Freyzon, E. Krementsova, K. A. Palmiter, M. J. Tyska, J. E. Baker, and K. M. Trybus. 2000. The light chain binding domain of expressed smooth muscle heavy meromyosin acts as a mechanical lever. *J. Biol. Chem.* 275:37167–37172.

Warshaw, D. M., E. Hayes, D. Gaffney, A. M. Lauzon, J. Wu, G. Kennedy, K. Trybus, S. Lowey, and C. Berger. 1998. Myosin conformational states determined by single fluorophore polarization. *Proc. Natl. Acad. Sci. U.S.A.* 95:8034–8039.

Weber, A., and J. M. Murray. 1973. Molecular control mechanism in muscle contraction. *Physiol. Rev.* 53:612–673.

Wells, A. L., A. W. Lin, L. Q. Chen, D. Safer, S. M. Cain, T. Hasson, B. O. Carragher, R. A. Milligan, and H. L. Sweeney. 1999. Myosin VI is an actin-based motor that moves backwards. *Nature.* 401:505–508.

Wilson, M. G. A., and R. A. Mendelson. 1983. A comparison of order and orientation of cross-bridges in rigor and relaxed muscle fibers using fluorescence polarization. *J. Musc. Res. Cell Mot.* 4:671–693.

Wolff-Long, V. L., L. D. Saraswat, and S. Lowey. 1993. Cysteine mutants of light chain-2 form disulfide bonds in skeletal muscle myosin. *J. Biol. Chem.* 268:23162–23167.

Xiao, M., O. A. Andreev, and J. Borejdo. 1995. Rigor cross-bridges bind to two actin monomers in thin filaments of rabbit psoas muscle. *J. Mol. Biol.* 248:294–307.

Yamamoto, K., and T. Sekine. 1983. Interaction of alkali light chain 1 with actin: effect of ionic strength on the %T cross-linking of alkali light chain 1 with actin. *J. Biochem.* 94:2075–2078.